

## Langmuir Sites in Semicrystalline Rubbery Films?

Vicente Compañ,<sup>†</sup> M. Mar López-González,<sup>‡</sup> and Evaristo Riande<sup>\*,‡</sup>

Departamento de Termodinámica, ETSII, Universidad Politécnica de Valencia, Valencia, Spain, and Instituto de Ciencia y Tecnología de Polímeros (CSIC), 28006 Madrid, Spain

Received May 27, 2003

Revised Manuscript Received August 6, 2003

In principle, the concentration of gases in rubbery polymers can be obtained from the change of free energy taking place in the mixture of the gas in liquid state with the molecular chains. According to the Flory–Huggins theory,<sup>1</sup> the variation of chemical potential arising from the mixture of a gas A in the liquid state with a polymer P can be written as

$$\frac{\mu - \mu_0}{RT} = \ln \frac{p_{A,T}}{p_{0A,T}} = \ln \phi_A + \phi_P \left( 1 - \frac{\bar{V}_A}{\bar{V}_P} \right) + \chi \phi_P^2 \quad (1)$$

where  $\phi_A$  and  $\phi_P$  are respectively the molar volume fractions of gas in liquid form and polymer so that  $\phi_A + \phi_P = 1$ ,  $\bar{V}_A$  and  $\bar{V}_P$  are the respective molar partial volumes, and  $p_{0A,T}$  and  $p_{A,T}$  represent respectively the vapor pressures of the gas in the liquid state and in solution at temperature  $T$ . By taking as reference the boiling point of the gas at 1 atm, the Clausius–Clapeyron equation allows to estimate  $p_{0A,T}$  at temperature  $T$  as

$$\ln p_{0A,T} = \frac{\lambda}{R} \left( \frac{1}{T_{bA}} - \frac{1}{T} \right) = \frac{\lambda}{RT_{bA}} \left( 1 - \frac{T_{bA}}{T} \right) \quad (2)$$

where  $\lambda$  is the latent heat of vaporization and  $T_{bA}$  is the boiling temperature of A under 1 atm of pressure. From eqs 1 and 2 it follows that<sup>2</sup>

$$\ln p_{A,T} = \ln \phi_A + \phi_P \left( 1 - \frac{\bar{V}_A}{\bar{V}_P} \right) + \chi_A \bar{V}_P^2 + \frac{\lambda}{RT_{bA}} \left( 1 - \frac{T_{bA}}{T} \right) \cong \ln \bar{V}_A c_A + (1 + \chi_A) - (1 + 2\chi_A) \bar{V}_A c_A + \frac{\lambda}{RT_{bA}} \left( 1 - \frac{T_{bA}}{T} \right) \quad (3)$$

where terms in  $\phi_A^2$  as well as the ratio  $\bar{V}_A/\bar{V}_P$  are neglected. It is also considered that  $\phi_A \cong \bar{V}_A c_A$ , where  $c_A$  is the molar concentration of gas in the liquid state in the polymer matrix. Hence, the solubility coefficient can be written as

$$S = c_A/p_{A,T} = k_D \exp(b'c_A) \quad (4)$$

where  $k_D$  is Henry's constant at temperature  $T$ , given by

$$k_D = \frac{22414}{76 \bar{V}_A} \exp[-(1 + \chi_A) - (\lambda/RT_{bA})(1 - T_{bA}/T)] \quad (5)$$

<sup>†</sup> Universidad Politécnica de Valencia.

<sup>‡</sup> Instituto de Ciencia y Tecnología de Polímeros (CSIC).

The units of  $\bar{V}_A$  and  $k_D$  in this expression are cm<sup>3</sup>/mol and cm<sup>3</sup> (STP)/(cm<sup>3</sup> cmHg), respectively. According to eq 5, the condensability of the gas and/or favorable polymer solvent interactions greatly enhance Henry's solubility constant. Moreover, the parameter  $b'$  in eq 4 can be written as

$$b' = (1 + 2\chi_A) \bar{V}_A \quad (6)$$

Since  $\chi_A \geq 0$  and  $T_{bA} < T$ ,  $S \geq k_D$ . On the other hand, at low pressures  $c_A \rightarrow 0$  and the sorption process follows Henry's solubility law. At high pressures,  $c_A$  may become significant so that the exponential term in eq 4 is not negligible. In this case, the isotherms representing the concentration of gas against pressure in rubbery polymers are concave with respect to the ordinates axis. This behavior has experimentally been observed in the sorption isotherms of CO<sub>2</sub> in poly(dimethylsiloxane).<sup>3</sup>

In this Note we report the sorption of carbon dioxide, oxygen, and nitrogen in linear low-density polyethylene (LLDPE) films containing 13 mol % octene. The degree of crystallinity of the film, estimated by DSC assuming the melting enthalpy of a pure crystal of polyethylene to be 960 cal/mol of CH<sub>2</sub>, amounts to ca. 0.25. The sorption process was monitored by measuring the decrease of the pressure of gas in a reservoir of 17.0 cm<sup>3</sup>, containing 6.22 g of polymer in film form. The pertinent expression used to obtain the concentration of gas in the films, in cm<sup>3</sup> of gas (STP)/cm<sup>3</sup> units, was

$$C = \frac{22414 V \rho}{mRT} \left( \frac{p_i}{z_i} - \frac{p_f}{z_f} \right) \quad (7)$$

where  $z_i$  and  $z_f$  represent respectively the compressibility of the gas at the initial,  $p_i$ , and final or equilibrium,  $p_f$ , pressures,  $\rho$  is the density of the polymer, and  $m$  is the mass of LLDPE film in the sorption chamber. The concentration thus calculated corresponds to the equilibrium pressure,  $p_f$ .

Values at 25 °C of the concentration of CO<sub>2</sub>, O<sub>2</sub>, and N<sub>2</sub> in the films are shown in Figure 1. At first sight, the concentration is a linear function of pressure, the correlation factor of the straight lines being larger than 0.99. From their slopes, the values of the apparent solubility coefficients in cm<sup>3</sup> (STP)/(cm<sup>3</sup> cmHg) units are  $1.63 \times 10^{-3}$ ,  $8.8 \times 10^{-4}$ , and  $4.3 \times 10^{-4}$  for CO<sub>2</sub>, O<sub>2</sub>, and N<sub>2</sub>, respectively. However, an attentive inspection of Figure 1 shows that the apparent straight lines do not intersect the coordinates axes at the origin, suggesting that the sorption processes do not strictly obey Henry's law. The results for the sorption coefficient,  $S = C/p$ , are plotted as a function of pressure in Figures 2, 3, and 4 for CO<sub>2</sub>, O<sub>2</sub>, and N<sub>2</sub>, respectively. It can be seen that the solubility coefficient in the low-pressure region sharply decreases, its value remaining nearly constant for values of  $p > 3$  bar.

The pressure dependence of the solubility of gases in LLDPE films, depicted in Figures 2–4, reminds one of that observed in glassy polymers. Sorption processes in glassy polymers have been interpreted in terms of the dual mode model that assumes the glassy matrix as formed by a continuous phase in which microcavities that account for the excess volume are dispersed. According to the model, gas solution in the continuous

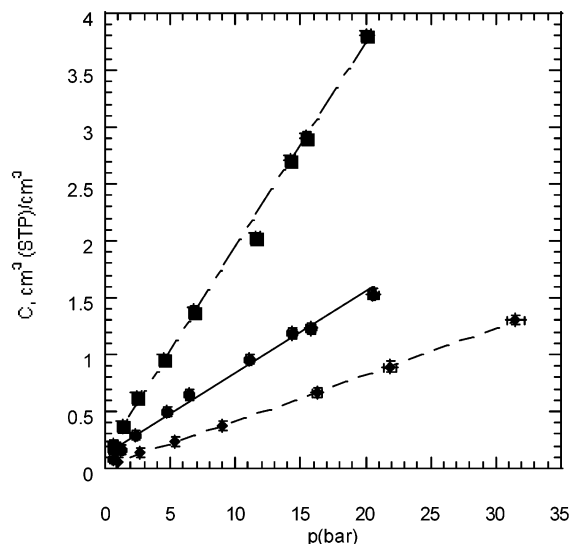


**Figure 1.** Variation of the concentration of CO<sub>2</sub> (■), O<sub>2</sub> (●), and (◆) N<sub>2</sub> in LLDPE films with pressure at 25 °C.

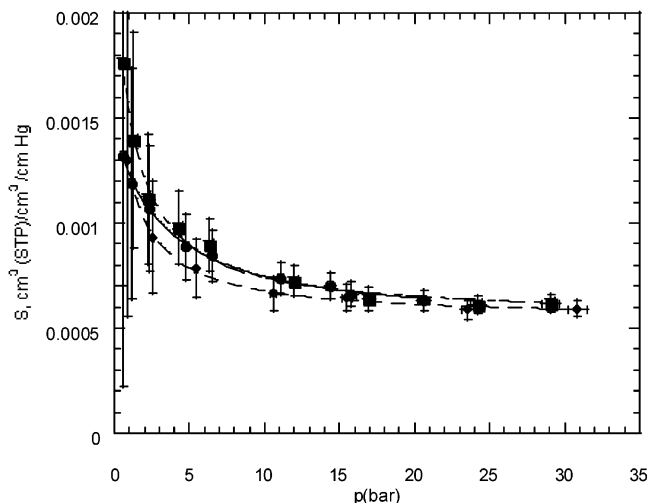


**Figure 2.** Dependence of the solubility coefficient of carbon dioxide in LLDPE films on pressure at 25 (●), 35 (■), and 45 °C (◆). Symbols represent experimental points whereas the curves were calculated using the dual mode parameters shown in Table 1.

phase obeys Henry's law whereas the microcavities act like Langmuir sites in which adsorption processes take place. The pertinent expression relating the solubility coefficient with pressure is<sup>4,5</sup>

$$S = k_D + \frac{C_H b}{1 + b p} \quad (8)$$

where  $k_D$  is the Henry's constant,  $C_H$  is the Langmuir concentration that accounts for the gas immobilized at the Langmuir sites, and  $b$  is a polymer–gas affinity parameter related to the sorption/desorption rates ratios. In general, the values of  $C_H$  tend to increase as the glass transition temperature increases. The plots of  $C_H$  against  $T_g - T$  for homologous series of polymers seem to fit to a straight line that intersects the coordinates axes at the origin.<sup>6</sup> This means that gas immobilization in the polymer matrix by effect of adsorption processes is a characteristic of the glassy state. However, the results of Figures 2–4 suggest that Langmuir sites seem also to be present in rubbery membranes containing crystalline entities in their

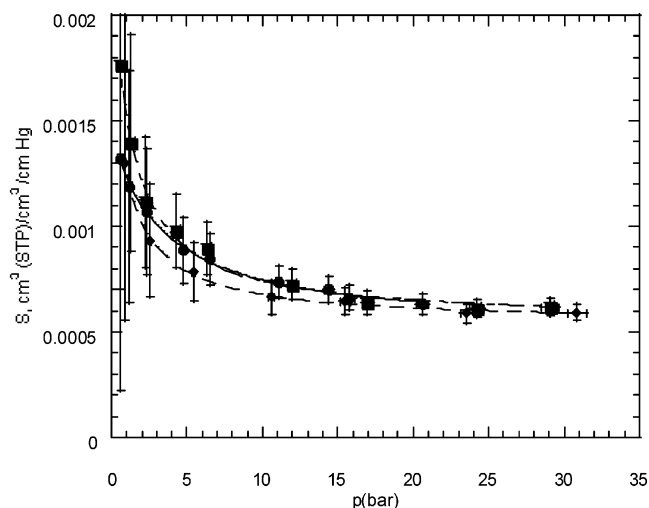


**Figure 3.** Variation of the solubility coefficient of oxygen in LLDPE films with pressure at 25 (●), 35 (■), and 45 °C (◆). Symbols represent experimental points whereas the curves were calculated using the dual mode parameters shown in Table 1.

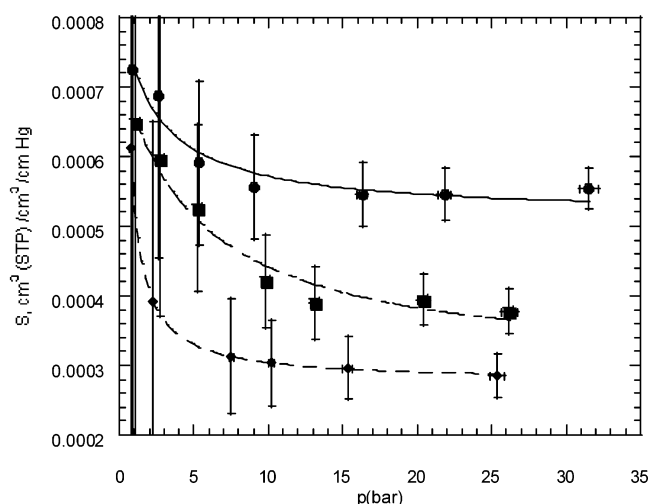


**Figure 4.** Dependence of the solubility coefficient of nitrogen in LLDPE films on pressure at 25 (●), 35 (■), and 45 °C (◆). Symbols represent experimental points whereas the curves were calculated using the dual mode parameters shown in Table 1.

structure since the solubility coefficients of carbon dioxide and oxygen decrease in nearly 50% in the interval 0.8–3 atm.

Values of the dual mode model parameters that fit the pressure dependence of the solubility coefficient of CO<sub>2</sub>, O<sub>2</sub>, and N<sub>2</sub> in LLDPE films are shown in Table 1. In general, the Langmuir concentration of gas in the films is significantly lower than that reported for glassy polymers where this parameter can reach values of up to 30 cm<sup>3</sup> (STP)/cm<sup>3</sup> or even more, depending on  $T_g$ . However, the values of  $b$  are higher than those reported for glassy polymers. As often occurs in glassy polymers,<sup>7</sup> the sorption processes of the gases in LLDPE films display exothermic character.

In an earlier work,<sup>8</sup> a decrease in the permeability coefficient of gases in LLDPE films at low pressures was reported. The fact that the diffusion coefficient was nearly insensitive to the upstream pressures led to conclude that the drop of the permeability coefficient with increasing pressure in the low-pressure region was

**Table 1.** Values of the Henry's Solubility Coefficient,  $k_D$ , the Langmuir Gas Concentration,  $C_H$ , and the Affinity Parameter,  $b$ 

| gas             | $T, ^\circ\text{C}$ | $10^3 k_D^a$     | $C_H^b$           | $b$ (cmHg)          |
|-----------------|---------------------|------------------|-------------------|---------------------|
| CO <sub>2</sub> | 25                  | $1.74 \pm 0.08$  | $0.76 \pm 0.13$   | $0.004 \pm 0.0007$  |
|                 | 35                  | $1.70 \pm 0.10$  | $0.41 \pm 0.12$   | $0.0135 \pm 0.0013$ |
|                 | 45                  | $1.64 \pm 0.05$  | $0.33 \pm 0.10$   | $0.0130 \pm 0.0003$ |
| O <sub>2</sub>  | 25                  | $0.95 \pm 0.06$  | $0.24 \pm 0.04$   | $0.0040 \pm 0.0010$ |
|                 | 35                  | $0.89 \pm 0.07$  | $0.15 \pm 0.05$   | $0.0122 \pm 0.0008$ |
|                 | 45                  | $0.88 \pm 0.03$  | $0.12 \pm 0.03$   | $0.0120 \pm 0.0008$ |
| N <sub>2</sub>  | 25                  | $0.54 \pm 0.014$ | $0.052 \pm 0.012$ | $0.006 \pm 0.002$   |
|                 | 35                  | $0.43 \pm 0.07$  | $0.078 \pm 0.02$  | $0.005 \pm 0.002$   |
|                 | 45                  | $0.41 \pm 0.08$  | $0.030 \pm 0.015$ | $0.0036 \pm 0.014$  |

<sup>a</sup> In cm<sup>3</sup> of gas (STP)/(cm<sup>3</sup> of polymer cmHg). <sup>b</sup> In cm<sup>3</sup> of gas (STP)/(cm<sup>3</sup> of polymer).

responsible for this at first sight anomalous behavior of the solubility coefficient. The values of the apparent solubility coefficients obtained from permeation experiments, in cm<sup>3</sup> (STP)/(cm<sup>3</sup> cmHg) units, were  $4.3 \times 10^{-3}$ ,  $2.1 \times 10^{-3}$ , and  $0.4 \times 10^{-3}$  for CO<sub>2</sub>, O<sub>2</sub>, and N<sub>2</sub> at 25 °C and 1 atm. These results are in rather good agreement with those of  $4.0 \times 10^{-3}$ ,  $1.2 \times 10^{-3}$ , and  $0.7 \times 10^{-3}$ , in cm<sup>3</sup> (STP)/(cm<sup>3</sup> cmHg) units, obtained from sorption measurements. Therefore, the present results support previous findings<sup>8</sup> concerning the similarity of semicrystalline rubbery membranes at low pressures, as far as the solubility of gases is concerned, with glassy membranes. However, the decrease of the solubility coefficient extends over a wider interval of pressure in glassy polymers due in great part to the low gas–polymer affinity in this state.

The high mobility of molecular chains in the amorphous phase of rubbery semicrystalline polymers rules out the presence of microcavities over long periods of time in this region. However, one could postulate the existence of microcavities or Langmuir sites in the crystalline–amorphous interface due to the fact that the motions in the interface are severely restricted. The presence of microcavities in defects of the crystalline entities can neither be ruled out. It is expected that a decrease in temperature will diminish chains mobility in the crystalline–amorphous interface, thus enhancing and consolidating the number of microcavities in the interface. The increase of the Langmuir capacity with decreasing temperature, shown in Table 1, supports this assumption.

Values of the boiling temperature under 1 atm of pressure, latent heat of vaporization, and the partial molar volume of carbon dioxide, oxygen, and nitrogen<sup>9–11</sup> are shown in Table 2. These quantities in conjunction with eq 5 were used to calculate Henry's constant at 25 °C, and the pertinent results for different values of the interaction parameters are given in Table 3. It can be seen that  $k_D$  decreases as  $\chi_A$  increases, and a reasonable agreement between calculated and apparent values of Henry's constant is achieved for CO<sub>2</sub> and O<sub>2</sub> for values of  $\chi_A = 1.7$  and 2.0, respectively. For N<sub>2</sub> the value  $\chi_A$  necessary to bring the calculated value of  $k_D$  to the

**Table 2.** Boiling Temperature under 1 atm of Pressure,  $T_b$ , Latent Heat of Vaporization,  $\lambda$ , and Partial Molar Volume,  $\bar{V}_A$ , for Carbon Dioxide, Oxygen, and Nitrogen

| gas             | $T_b, ^\circ\text{C}^a$ | $10^{-3}\lambda$ , cal/mol <sup>a</sup> | $\bar{V}_A$ at $T_b$ , cm <sup>3</sup> /mol <sup>b</sup> |
|-----------------|-------------------------|---|--|
| CO <sub>2</sub> | −78.5                   | 6.063                                   | 45   |
| O <sub>2</sub>  | −182.9                  | 1.629                                   | 28   |
| N <sub>2</sub>  | −195.6                  | 1.333                                   | 35   |

<sup>a</sup> Reference 9. <sup>b</sup> References 10 and 11.

**Table 3.** Variation of  $k_D$  with the Values of the Interaction Parameter  $\chi_A$  at 25 °C

| $\chi_A$ | $10^3 k_D$ , CO <sub>2</sub> <sup>a</sup> | $10^3 k_D$ , O <sub>2</sub> <sup>a</sup> | $10^3 k_D$ , N <sub>2</sub> <sup>a</sup> |
|----------|---|--|--|
| 0        | 10.4                                      | 6.8                                      | 5.1                                      |
| 0.5      | 6.3                                       | 4.1                                      | 3.1                                      |
| 1.0      | 3.8                                       | 2.5                                      | 1.9                                      |
| 1.5      | 2.3                                       | 1.5                                      | 1.1                                      |
| 2.0      | 1.4                                       | 0.9 <sub>2</sub>                         | 0.6 <sub>9</sub>                         |
| 2.5      | 0.8 <sub>5</sub>                          | 0.5 <sub>6</sub>                         | 0.4 <sub>1</sub>                         |
| 3.0      | 0.5 <sub>2</sub>                          | 0.3 <sub>4</sub>                         | 0.2 <sub>5</sub>                         |

<sup>a</sup> In cm<sup>3</sup>(STP)/(cm<sup>3</sup> cmHg).

experimental result lies in the vicinity of 3. Given the relative proximity of the boiling points of oxygen and nitrogen, the low solubility of nitrogen in comparison with oxygen is mostly due to the polymer–gas interaction, which is very unfavorable for nitrogen. However, the differences between Henry's constant of carbon dioxide and oxygen are mainly caused by the considerable difference of condensability of the two gases.

Summing up, the isotherms representing the pressure dependence of the solubility coefficient of gases in semicrystalline polymers are described by the dual mode model. These systems present lower Langmuir gas concentration, but higher gas–polymer affinity, than glassy polymers. The good concordance of the calculated values of  $k_D$  with the experimental results suggests that the expression obtained for Henry's constant, using the Flory–Huggins theory of polymer diluent mixtures, may be a suitable way to estimate polymer–gas enthalpic interactions.

## References and Notes

- (1) Flory, P. J. *Principles of Polymer Chemistry*; Cornell University Press: Ithaca, NY, 1953.
- (2) Petropoulos, J. H. *Pure Appl. Chem.* **1993**, *65*, 219.
- (3) Fleming, G. K.; Koros, W. J. *Macromolecules* **1986**, *19*, 2285.
- (4) Vieth, W. R.; Sladek, K. J. *J. Colloid Sci.* **1965**, *20*, 1014.
- (5) Kesting, R. E.; Fritzsche, A. K. *Polymeric Gas Separation Membranes*; Wiley-Interscience: New York, 1993; p 60.
- (6) Yampolskii, Yu. P.; Shishatskii, S.; Alentiev, A.; Loza, K. *J. Membr. Sci.* **1998**, *149*, 203.
- (7) van der Vegt, N. F. A. *J. Membr. Sci.* **2002**, *205*, 125.
- (8) Compañ, V.; López-Lidón, M.; Andrio, A.; Riande, E. *Macromolecules* **1998**, *31*, 6984.
- (9) *International Critical Tables*, Vol. III, 1928.
- (10) Merkel, T. C.; Bondar, V. I.; Nagai, K.; Freeman, B. D.; Pinnau, I. *J. Polym. Sci., Part B: Polym. Phys.* **2000**, *38*, 415.
- (11) Kamiya, I.; Naito, Y.; Mizoguchi, K.; Terada, K.; Moreau, J. *J. Polym. Sci., Part B: Polym. Phys.* **1997**, *35*, 1049.

MA030287V